Construction of nano-assembly for mild photothermal therapy of tumors

Shi Sun, Xianfeng Zhou*

College of Polymer Science and Engineering, Qingdao University of Science and Technology, Qingdao, 266042, P.R. China.

Abstract. Due to the high incidence and mortality rates of cancer, it is necessary to seek more targeted and effective treatment methods. Traditional cancer treatment methods have problems such as incomplete treatment and significant side effects. In recent years, photothermal therapy (PTT) has been considered one of the most promising treatment methods in the biomedical field. The treatment principle of PTT is to use materials with high photothermal conversion efficiency to absorb near-infrared light (NIR) and generate heat to ablate tumors. PTT has the advantages of low toxicity, non-invasiveness, strong specificity, and high controllability. However, the self-protective mechanism related to heat shock proteins (HSPs) gives cancer cells thermal tolerance. To minimize the thermal tolerance of cancer cells and improve the efficacy of PTT, a nano-assembly composed of Pluronic F-127 encapsulating the HSP inhibitor APO and the high photothermal conversion efficiency photosensitizer Cy7-TCF has been developed. The nano-assembly can accumulate at the tumor site and generate heat under near-infrared light irradiation. At the same time, it inhibits the expression of heat shock proteins, achieving the effect of mild photothermal therapy and reducing thermal damage to surrounding tissues.

1. Introduction

Cancer still poses a threat to human health today, and research on cancer treatment is of great significance. Traditional cancer treatment methods often fail to achieve the expected therapeutic effects. Photothermal therapy (PTT) is an emerging tumor treatment method that has many advantages [1]. However, PTT still faces some issues that need to be addressed. When the temperature is in the thermal therapy range, excessive temperature under laser irradiation can initiate the self-protection mechanism of cells, inducing the overexpression of heat shock proteins (HSPs) [2]. The excessive production of HSPs enhances the heat stress response of tumor cells, making them thermally tolerant and significantly reducing the efficacy of PTT [3]. At the same time, uncontrolled heat diffusion can also pose a threat to surrounding healthy tissues.

Heat stress or heat shock proteins (HSPs) are a group of highly conserved proteins that are induced to be expressed when the physiological environment is violated, such as antitumor therapy (chemotherapy, PTT, etc.), protecting cells from harsh environments [4]. HSP70 is an important molecular chaperone in the HSP family and is closely related to tumor therapy, with high expression in tumor sites [5]. Therefore, various HSP70 inhibitors have been developed for tumor therapy. It has been found that Apoptozole (APO) has a strong inhibitory effect on HSP70 and Hsc70 [6]. The combination of APO and photothermal PS can significantly improve the PTT efficacy by overcoming the heat resistance of tumor cells and achieving mild PTT. Therefore, the development of a nano-assembly that simultaneously encapsulates photosensitizers and HSP inhibitors can minimize thermal resistance, reduce the heat resistance of tumor cells, effectively inhibit cancer cells at mild temperature conditions (45°C), improve the efficacy of PTT at tumor sites, and reduce heat damage to surrounding tissues.

2. Experiments

Synthesis of heat shock protein inhibitor APO: 3,5-Bis (trifluoromethyl) benzaldehyde, ammonium acetate, 4-(aminomethyl) benzoic acid, 1,2-bis (4-methoxyphenyl) ethane-1,2-dione were added to acetic acid and stirred at 100°C for 15 hours. The reaction was cooled to room temperature, then 2-Aminoethanol was added and the reaction was stirred at room temperature for 12 hours. The reaction mixture was concentrated by rotary evaporation and purified by column chromatography to obtain a yellow oily compound.

Synthesis of photosensitizer Cy7-TCF: Compound 8 was prepared by stirring 3-hydroxy-3-methyl-2-butanone, acetonitrile, ethyl magnesium bromide, and anhydrous ethanol as the solvent overnight at 60°C. Then, compound 10 was prepared by adding phosphorus oxychloride and cyclohexanone to a solution of anhydrous dichloromethane and stirring at 80°C for 3 hours. Compound 11 was obtained by dissolving compound 10 and compound 8 in anhydrous ethanol and reacting at 90°C for 12 hours. Compound 14 was obtained by adding 2,3,3-trimethyl-3H-indolenine and 2-iodoethanol to

* Corresponding author: xianfeng@qust.edu.cn

anhydrous acetonitrile and reacting at 100°C for 14 hours. Compound 15 was obtained by adding compound 11 and compound 14 to anhydrous ethanol and reacting at room temperature for 12 hours.

Synthesis of Nano-assembly APO/Cy7-TCF@F127: Equal amounts of PluronicF-127, a photosensitizer (compound 15), and HSP inhibitor (compound 5) were stirred at 37°C for 12 hours to obtain the nano-assembly APO/Cy7-TCF@F127 by physical encapsulation.

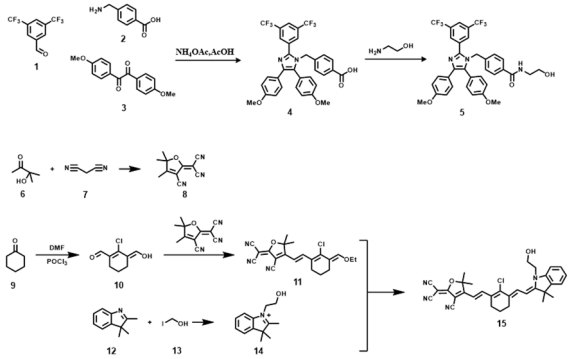

Figure 1. Synthesis of Nano-assembly APO/Cy7-TCF@F127.

3. Results and discussion

3.1 Photophysical characteristics

A 2 mM storage solution of APO/Cy7-TCF@F127 was added to different organic solvents to prepare samples with a concentration of 10 μM.

The UV-Vis absorption spectra and fluorescence emission spectra were measured by adding the samples to quartz cuvettes. The UV-Vis absorption spectra of APO/Cy7-TCF@F127 in different solvents are shown in Fig. 2(a). The strongest UV absorption of APO/Cy7-TCF@F127 was observed in acetonitrile, with maximum absorption at 834 nm. The UV absorption intensity in water was the weakest, with a broadened absorption peak and a red shift of the maximum absorption peak to 860 nm, indicating that APO/Cy7-TCF@F127 dispersed in organic solvents has good solubility and dissolves in the form of molecules in organic solvents.

The fluorescence emission spectra of the nano-assembled APO/Cy7-TCF@F127 were tested in different solvents as shown in Fig. 2(b). The maximum emission peak appeared in methanol at 865 nm, while the fluorescence emission peak was weakest in water due to fluorescence quenching. The differences in UV and fluorescence spectra observed in different solvents and water were attributed to the different aggregation structures in water.

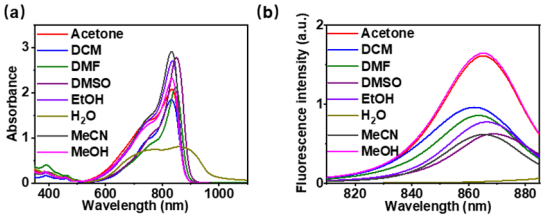

Figure 2. (a) UV absorption spectra in different organic solvents. (b) Fluorescence spectra in different organic solvents.

3.2 Self-assembly characterization

After the successful synthesis of the target product nano-assembly, we tested the particle size of the nano-assembly and its distribution using dynamic light scattering tests and transmission electron microscopy.

APO/Cy7-TCF@F127 was prepared into a sample with a concentration of 10 μM and added to a transparent quartz cuvette for DLS testing. The results of the DLS test are shown in Fig. 3(a), which indicated that APO/Cy7-TCF@F127 formed nano-aggregates with an average hydrodynamic diameter of approximately 100 nm in the aqueous solution. The average hydrodynamic diameter did not change significantly after being placed in water for 24 hours, indicating that APO/Cy7-TCF@F127 can self-assemble into stable nanostructures in aqueous solutions with good structural stability.

The transmission electron microscopy (TEM) sample of APO/Cy7-TCF@F127 was prepared using the dropwise method. The sample was prepared at a concentration of 10 μM and 10 μL was added to a copper grid, which was then placed in the dark overnight to allow the water to evaporate before TEM testing. The TEM results, as shown in Fig. 3(b), indicate that APO/Cy7-TCF@F127 nano-assemblies had good dispersion and circular structures. The TEM results showed that the diameter of APO/Cy7-TCF@F127 nanoparticles in water was approximately 150 nm, which was consistent with the DLS data. This further demonstrated that APO/Cy7-TCF@F127 can form aggregates and self-assemble into nanoparticles in aqueous solutions.

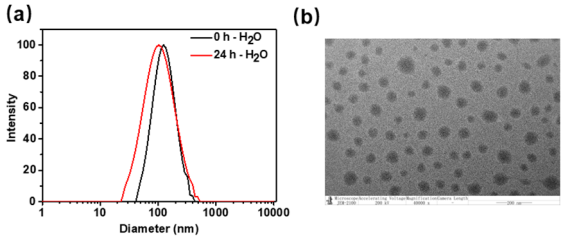

Figure 3. (a) DLS size profiles of APO/Cy7-TCF@F127. (b) TEM images of APO/Cy7-TCF@F127 in water.

3.3 Photothermal effect test

The photothermal effect is a key factor in testing the anti-tumor effect of photothermal therapy. Therefore, the in vitro photothermal effect of APO/Cy7-TCF@F127 nanoparticles was tested. Firstly, the sample was prepared by taking the storage solution of APO/Cy7-TCF@F127 and preparing samples with different concentrations. The APO/Cy7-TCF@F127 sample was placed in a transparent quartz cuvette and then irradiated with an 808 nm laser. The temperature was monitored and recorded using a photothermal imaging system.

Samples of APO/Cy7-TCF@F127 with concentrations of 10 μM, 20 μM, and 25 μM were prepared, with water as the control group. All samples were irradiated with an 808 nm laser at the same power (1.5 W/cm^2) for 10 minutes, as shown in Fig. 4(a). The temperature of the 25 μM sample increased by 25.1°C, the temperature of the 20 μM sample increased by 17.7°C, the temperature of the 10 μM sample increased by 14.1°C, and the temperature of the pure water sample increased by 1.2°C (the temperature change can be ignored). The photothermal heating effect improved as the sample concentration increased, indicating that APO/Cy7-TCF@F127 has good photothermal effects.

Then, the photothermal stability of APO/Cy7-TCF@F127 was tested. APO/Cy7-TCF@F127 was prepared as a sample with a concentration of 25 μM, and a laser was used to irradiate the sample for 10 minutes. The temperature change was recorded every 10 seconds, and then the laser was stopped to allow natural cooling for 15 minutes. The temperature change during cooling was recorded every 30 seconds. The sample was subjected to 5 cycles of heating and cooling under unchanged conditions. The temperature change is shown in Fig. 4(b), and the temperature-time curve and peak shape did not show any significant changes after the cyclic heating and cooling process, indicating that APO/Cy7-TCF@F127 has good photothermal stability.

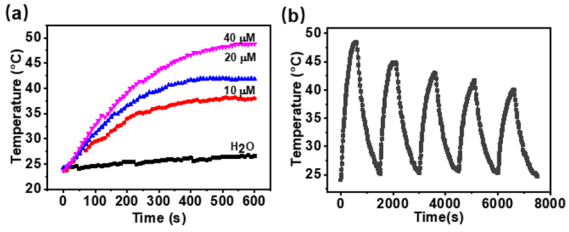

Figure 4. (a) Temperature rise curves of APO/Cy7-TCF@F127 at different concentrations. (b) Photothermal stability of APO/Cy7-TCF@F127.

3.4 In vitro cell photothermal performance

The Live/Dead staining method was used to test the cytotoxicity of APO/Cy7-TCF@F127 and its killing effect on tumor cells. Live and dead cells were stained with Calcein-AM (green) and EthD-1 (red), respectively. As shown in Fig. 5(a), the unirradiated nano-assembly appeared green, and almost all HeLa cells survived. In contrast, the nano-assembly irradiated with the laser caused all HeLa cells to die due to photothermal therapy. This indicates that the APO/Cy7-TCF@F127 used for photothermal therapy has an excellent killing effect on tumor cells under laser irradiation.

To ensure the biosafety of APO/Cy7-TCF@F127 nanoparticles, the anti-tumor activity of APO/Cy7-TCF@F127 was further quantitatively studied in HeLa cells using the MTT assay, as shown in Fig. 5(b). The APO/Cy7-TCF@F127 sample showed almost no toxicity to cells without laser irradiation. After irradiation with an 808 nm laser, APO/Cy7-TCF@F127 exhibited phototoxicity. At a concentration of 0.4 μM, there was a certain degree of tumor-killing effect (93.5%), and at a concentration of 12.5 μM, all tumor cells could be killed. This indicates that APO/Cy7-TCF@F127 has good biosafety, low dark toxicity, and phototoxicity that increases proportionally with sample concentration.

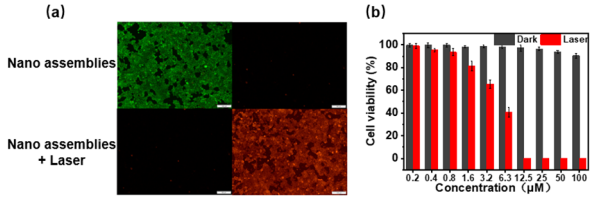

Figure 5. (a) Fluorescent live/dead cell images of HeLa cells. (b) Cell viability after incubating cells with different concentrations of APO/Cy7-TCF@F127.

4. Conclusion

A nano-assembly was synthesized by encapsulating a heat shock protein inhibitor APO and a photosensitizer Cy7-TCF in Pluronic F-127, which can target the tumor site through the EPR effect after self-assembly. APO/Cy7-TCF@F127 exhibits good photothermal effect and photothermal stability, enabling the precise killing of tumor cells. At the same time, the heat shock protein inhibitor reduces the heat resistance during photothermal therapy by down-regulating the production of heat shock proteins, enhancing the photothermal therapy effect, reducing thermal damage to surrounding healthy tissues, and enabling the mild ablation of tumors at a moderate temperature.

References

1. Doughty A, Hoover A, Layton E, Nanomaterial Applications in Photothermal Therapy for Cancer. Materials 2019, 12 (5), 779-793.
2. Wang P, Chen B, Zhan Y, Enhancing the Efficiency of Mild-Temperature Photothermal Therapy for Cancer Assisting with Various Strategies. Pharmaceutics 2022, 14 (11), 110391.
3. Gao P, Wang H, Cheng Y, Strategies for efficient photothermal therapy at mild temperatures: Progresses and challenges. Chinese Chemical Letters 2022, 33 (2), 575-586.
4. Albakova Z, Mangasarova Y, Albakov A, HSP70 and HSP90 in Cancer: Cytosolic, Endoplasmic Reticulum and Mitochondrial Chaperones of Tumorigenesis. Frontiers in Oncology 2022, 12 (17), 829520.

5. Cui X, Liang Z, Lu J, A multifunctional nanodiamond-based nano platform for the enhanced mild-temperature photothermal/chemo combination therapy of triple negative breast cancer via an autophagy regulation strategy. Nanoscale 2021, 13 (31), 13375-13389.
6. Ren Y, Chen Q, Qi H, Experimental Comparison of Photothermal Conversion Efficiency of Gold Nanotriangle and Nanorod in Laser Induced Thermal Therapy. Nanomaterials 2017, 7 (12), 416-430.